MODELLING OF SPUR GEAR CONTACT USING A LOCAL ADAPTIVE FINITE ELEMENT MESH

J. Lahtivirta[1*], A. Lehtovaara[1]

[1]Group of Tribology and Machine Elements, Materials Science: Tampere University of Technology
P.O. BOX 589 33101 Tampere, Finland
* Corresponding author: Juuso Lahtivirta (juuso.lahtivirta@tut.fi)

ABSTRACT

The gear drive is a critical part of a power transmission system. Modelling and simulating of the gear pair with finite element method (FEM) take important role as a part of the design process to estimate stresses, deformations, and damage risks in various operating conditions. A parameterized calculation model for the analysis of stresses in the gear contact and the gear root was developed. A local adaptive FE mesh was used, where a dense FE mesh zone around the contact point moves along the line of action to speed up the computation. The adaptive FE mesh, the rotation of the gear pair, and the accurate surface profile based on gear hobbing process were created in Matlab environment to obtain a good control of the flank profile and the meshing parameters. These were integrated with a commercial FEM software to calculate deformations and stresses. The developed FE mesh approach was validated successfully against analytical Hertzian theory. In addition, the developed spur gear model was compared to the gear standard ISO 6336 and a commercial gear calculation software resulting in relatively good correspondence with the maximum contact pressure and the maximum tooth root stresses.

INTRODUCTION

The gear drive is a critical part of a power transmission system which transfers the required torque by tooth mesh. Current demands need improvement of energy efficiency and power density, which require components and structures with minimized mass and dimensions. To satisfy these needs, modelling and simulating of the gear pair take important role as a part of the design process to estimate stress distributions and damage risks of the gear tooth in various operating conditions.

To achieve a realistic model of the gear contact, the geometry of the gear flank profile has to be accurate. Litvin et al. [1] presented a paper in which the gear surface is determined as the envelope to the family of rack-cutter surfaces. Hedlund and Lehtovaara [2, 3] used the same method. In their solutions, coordinate conversions are used to form an accurate geometry of the gear imitating the gear manufacturing i.e. the hobbing process. In addition, Hedlund and Lehtovaara set the geometry data to a certain matrix form, which can be utilized in the FE calculation, by using synchronization.

The exact simulation of the gear contact is challenging. Several studies of the gear systems have been done by using multibody approaches, in which the gear contact is simulated using simplified models to avoid the high computational efforts. Ebrahimi and Eberhard [4] used a rigid-elastic multibody approach to model the gear contact. In their study the elastic element simulates the flexibility of the tooth. Do et al. [5] used the elastic multibody approach for simulation of elastic gears with non-standard flank profiles.

However, when the stress distribution in gear flank and tooth root is studied thoroughly finite element method (FEM) is required. In gear pair with non-conformal surfaces, the contact is localized in a very small area so that very dense FE mesh is needed to achieve a good accuracy. The challenge is to reduce the number of elements so that the accuracy is preserved. Gonzalez-Perez et al. [6] proposed a FE model which has better control of the FE mesh refinement around the contact point. In their solution, the contact area is refined, so that the size of the element in the contact area is smaller than elsewhere in the model. Barbieri et al. [7] presented a paper in which the problem was solved using adaptive grid-size finite element modelling. In this solution, the Non Uniform Rational Basis Spline (NURBS) description allows to use iterative FE mesh refinement during numerical solution, and attach the new nodes to the mathematical surface.

In this paper, a parameterized calculation model for spur gear contact analysis is introduced. The FEM is used to calculate deformations and stress distributions. The FE mesh consists of two parts, which enables a dense FE mesh around the contact point and a sparse FE mesh elsewhere aiming for a faster model with reasonable accuracy. The developed FE mesh approach is validated against analytical Hertzian theory and the results of the developed spur gear model are compared to the results of the gear standard ISO 6336 and the commercial gear calculation software.

GENERATION OF GEOMETRY

The used method for generating the gear flank geometry simulates the gear manufacturing i.e. the hobbing process. The approach is based on the wide group of the digital calculation points and their synchronization, which allows the parametrization of the geometry and the divergences from ordinary involute shape without curve fitting [2, 3]. As an example of gearing, coordinate systems S_1 and S_2 are rigidly connected to the gear and the rack-cutter, respectively. The rack-cutter performs rotational and translational motions with respect to the fixed coordinate system S_g, as shown schematically in Fig. 1.

Profile of the gear in the coordinate system S_1 is obtained with the inverse of the transformation matrix $\boldsymbol{M}_{21}$ that is a multiplication of a rotation matrix and a translation matrix. The rotation matrix $\boldsymbol{M}_{g1}$ describes rotation about the z_g axis and the translation matrix $\boldsymbol{M}_{2g}$ describes translation from the coordinate system S_g to S_2. The transformation matrix $\boldsymbol{M}_{12}$ in cylindrical involute gear case is represented in Eq. (1),

$$\boldsymbol{M}_{12} = \boldsymbol{M}_{21}^{-1} = \begin{bmatrix} \cos(\emptyset) & \sin(\emptyset) & 0 & \sin(\emptyset)r_{w1} + \sin(\emptyset)h_1 - \cos(\emptyset)\, r_{w1}\emptyset \\ -\sin(\emptyset) & \cos(\emptyset) & 0 & \cos(\emptyset)r_{w1} + \cos(\emptyset)\, h_1 + \sin(\emptyset)r_{w1}\emptyset \\ 0 & 0 & 1 & 0 \\ 0 & 0 & 0 & 1 \end{bmatrix} \quad (1)$$

where r_{w1} is the pitch radius of the pinion and the addendum modification is taken into account using coefficient h_1. Transformation matrix $\boldsymbol{M}_{12}$ describe a rack-cutter rolling without sliding around the pitch circle of the gear. More details about the generation of involute curves by tools can be found in [8].

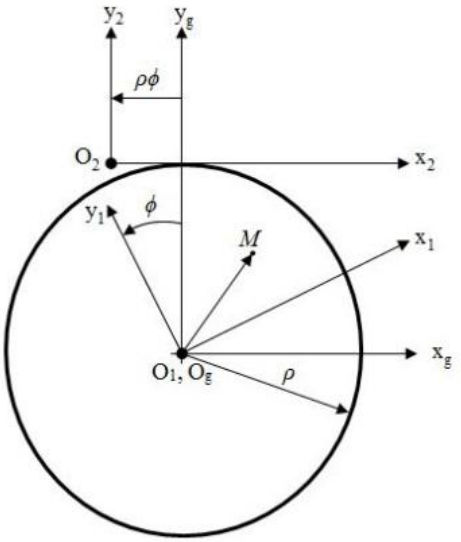

Fig. 1. Rotational and translational motions with respect to the fixed coordinate system.

The tooth profile is formed according to the SFS standard [9]. The geometry is determined using synchronization [3]. With the synchronization the geometry data can be set to a certain matrix form. In this case three-dimensional geometry matrices are correctly formulated for establishing the FE mesh that is important in this work.

GEAR CONTACT ALONG THE LINE OF ACTION

The meshing of a pair of involute spur gear teeth is shown in Fig. 2. The gears rotate around centres O_1 and O_2. The line C_1C_2 is the line of action which is the common tangent to the base circles. The points in the beginning (point *A*) and at the end (point *B*) of meshing define the working part of the line of action. These points are obtained as points of intersection of the line of action with the respective tip circles. [8.] *P* is the pitch point where the pitch circles touch each other. The teeth are shown in contact at point *C*. In gear contact, the point of contact moves along the line of action when the gears are rotated around their centres. Because of the continuity of contact, the surfaces are neither separating nor overlapping, the velocity components along the line of action must be equal [10].

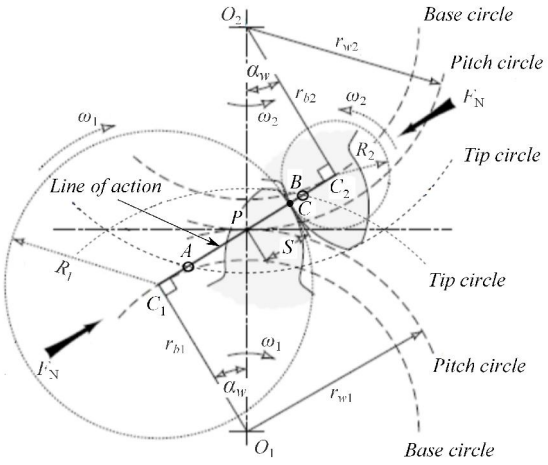

Fig. 2. Contact of involute spur gear teeth (*modified from* [11]).

It is possible to model any specific contact position on the tooth surface of an involute gear by two rotating cylinders, as shown in Fig. 2. The radii of the cylinders can be defined by Eq. (2),

$$\left.\begin{aligned} R_1 &= r_{w1}\sin\alpha_w + S \\ R_2 &= r_{w2}\sin\alpha_w - S \end{aligned}\right\} \qquad (2)$$

where α_w is the working pressure angle, S is the distance of the point of contact from the pitch point, r_{w1} and r_{w2} are the pitch circle radii. Subscripts 1 and 2 indicate that variables are related to the pinion and the gear, respectively. The distance S is continuously changing with the contact position during the meshing cycle of the gears.

CONTACT MODEL

In this work, a geometry of the spur gear tooth and a FE mesh for a finite element model are created using MATLAB software. In that way, the size and numbering of elements can be controlled irrespective of FEM software.

A main idea of this model is to use so called moving contact FE mesh formulation in which the dense part of the FE mesh moves when the point of contact changes along the line of action. The FE mesh is formed so that the element size is small only nearby the contact area, which enables a faster model with reasonable accuracy. A flow chart for the calculation procedure is shown in Fig. 3.

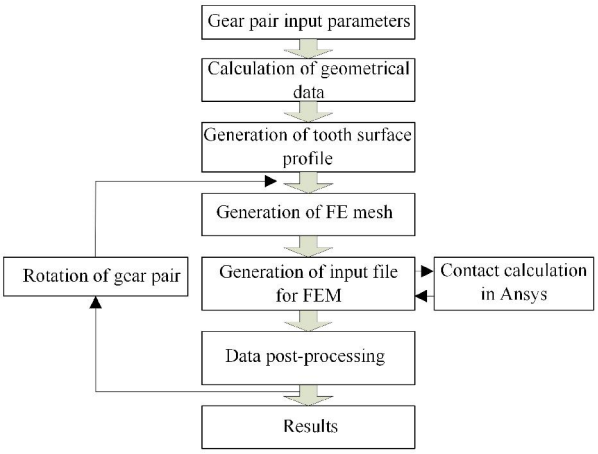

Fig. 3. Flow chart for the calculation procedure.

A tooth surface profile is created in MATLAB by simulating the gear manufacturing i.e. the hobbing process as described above. The selected points of the calculated surface profile are used to generate the FE mesh of the tooth. The FE mesh consists of two parts (a dense part and a coarse part), as shown in Fig. 4 with different colours. That allows more effective reduction of the FE mesh density in the locations which are not close the contact area. The displacements between contacting surfaces of the two parts are “tied” together using Multi-Point constraint (MPC) contact formulation [12].

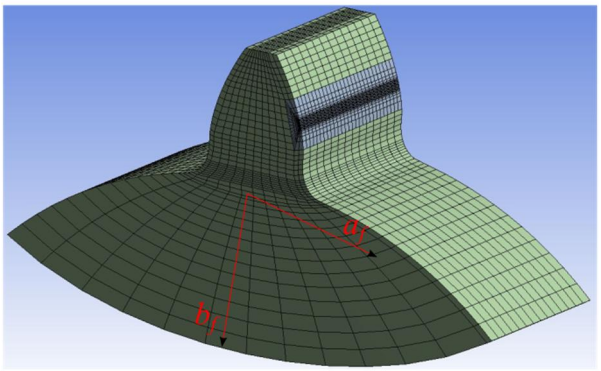

Fig. 4. The FE Mesh of the gear tooth which consists of two parts.

The FE mesh creation is parameterized. In the coarse part of the FE mesh, the number of elements in the tooth thickness direction and the tooth height direction stay constant and are controlled with separate parameters. In addition, the number of elements in the tooth root region can be separately changed in the height direction. The foundation mesh (the mesh below the tooth) is created using elliptical shape to generate the FE mesh boundaries. The semi-axes of the ellipse, a_f and b_f (see Fig. 4), can be used as parameterized variables to vary the form of the semi-elliptical foundation [13]. The number of elliptical lines can be also varied.

The parameterization of the FE mesh refinement around the contact point (the dense part) is based on the half of the contact width b using seven parameters (L_c, H_c, n_{mesh}, n_{side}, b_{side}, c_{side}, and n_{axial}). The contact width b is predicted using Hertzian theory (contact between two cylinders with parallel axes). A size of the dense part is defined using parameters L_c and H_c, which are the width and height of the dense part, respectively. Parameter n_{mesh} is the number of elements that covers dimension 2*b around the initial contact point. The size of the elements in contact region may be obtained as $Mesh\ size = 2 * b/n_{mesh}$. Parameter n_{side} defines the number of elements which are added along dimension b, right and left. This establishes the number of elements in the contact region as $a_{cont} = n_{mesh} + 2 * n_{side}$. The numbers of elements beside the contact region and at the edge of the dense part are controlled by parameters b_{side} and c_{side}, respectively. The number of elements in the face width (axial) direction is controlled by parameter n_{axial}.

A simplified example of the FE mesh refinement is shown in Fig. 5, where one block corresponds to one element. In practice the amount of elements in this defined area is much higher.

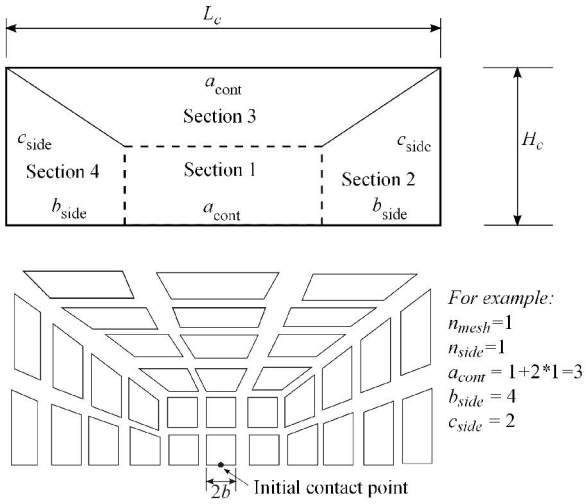

Fig. 5. Schematic illustration of the arrangement for the FE mesh around the contact point.

The contact point is changing along the line of action when gear pair is rotated. This contact point and the corresponding contact width can be determined separately in each rotation step. In each rotation step, the tooth moves along the line of action and the FE mesh of the pinion and gear are automatically

updated i.e. the dense part of the FE mesh follows the contact point, as illustrated in Fig. 6.

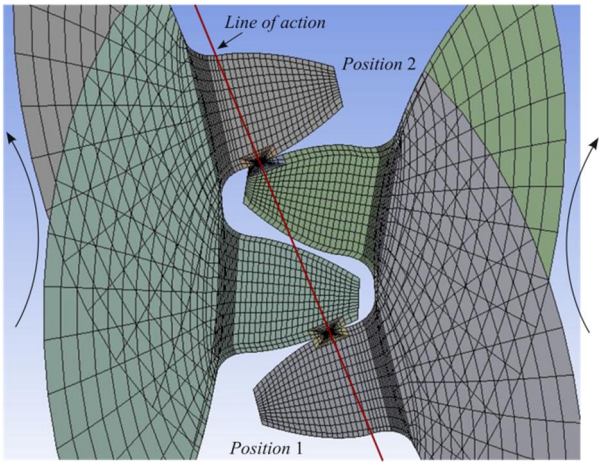

Fig. 6. Illustration of the moving dense part of the FE mesh with two different positions of the contact (single gear pair in contact).

Nodes on the bottom part of the gear rim are encastred using fixed support. A reference node *N* (Pilot Node) located on the axis of the pinion is used as the reference point of the bottom part of the pinion rim defined as a rigid surface. The reference point *N* and the rigid surface constitute a rigid body, as shown in Fig. 7.

A rotation degree of freedom (DOF) about the pinion *x* axis is defined as free at the reference point *N* while all other DOFs are fixed. A moment M_1 at the reference point *N* allows applying such a moment to the pinion model while the gear model bottom part is fixed.

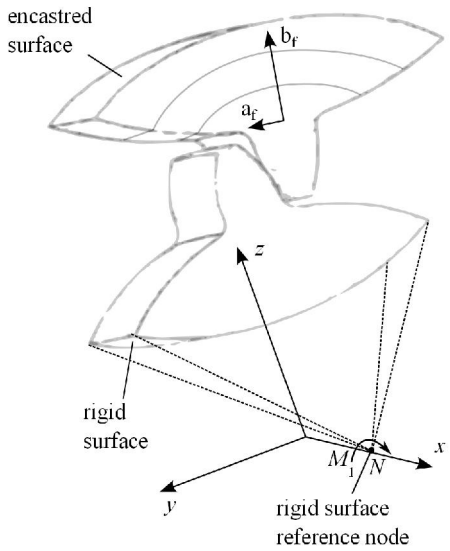

Fig. 7. Schematic illustration of: boundary conditions for the pinion and the gear, reference node of the rigid surface of the pinion, and the tooth foundation.

Frictionless contact is used between gear pair. Contact is modeled as flexible-flexible contact in which both contact (pinion) and target (gear) surfaces are associated with deformable bodies. The used element type is 4-node surface-to-surface contact element which is located on the surface of 3D solid element (eight-node trilinear hexahedral elements). It has the same geometric characteristics as the underlying elements [12].

Augmented Lagrangian Method is used as contact algorithm. It leads to better conditioning and is less sensitive to the magnitude of contact stiffness coefficient than penalty method for example [12].

RESULTS AND VALIDATION OF THE DEVELOPED FE MESH APPROACH

Contact between two cylinders, which can be used to represent a single contact position in gear mesh, was used to test the developed FE mesh approach. The calculated results were validated against Hertzian theory so that the required FE mesh density could be determined. The validation of the FE mesh approach was done in two parts. Two-dimensional (2D) contact of cylindrical bodies was used to test the effect of the different FE mesh parameters on contact pressure, maximum shear stress, and equivalent (Von Mises) stress. The effect of the FE mesh density in axial direction on contact pressure, and maximum shear stress was studied using three-dimensional (3D) model.

Two-dimensional contact of cylindrical bodies

The gear pair geometry considered in this test case is shown in Table 1. The contact at the pitch point was chosen as a situation to be examined.

Radii of the cylinders which represent the contact in the pitch point were calculated using Eq. (2). The cylinders were pressed against each other with a normal load which correspond the nominal transverse tangential force at the pitch cylinder (F_N in Fig. 2). Boundary conditions of the cylinders and a reference node of a rigid surface of the cylinder were defined according to the spur gear model described above. In this case, a displacement DOF along the *y* axis was defined as free at the reference point while all other DOFs were fixed. The normal load was applied to the reference node. Correspondingly, the FE meshes of the cylinders consisted of two parts, the dense part and the coarse part. The dense part was created as described above.

Table 1. Common gear data for a spur gear drive and other input parameters.

	Pinion		Gear
Number of teeth, Z_1, Z_2	16		24
Module, m_n [mm]		4.5	
Pressure angle, α_n [deg]		20	
Helix angle,β_0 [deg]		0	
Addendum modification factor, x_1, x_2 [mm]	0.182		0.171
Face width, b_{width} [mm]	14		14
Tip circle of the pinion, d_{a1}, d_{a2} [mm]	82.45		118.35
Centre distance, a_{cent} [mm]		91.5	
Elastic modulus, E [Pa]		$210\text{x}10^9$	
Poisson's ratio, υ		0.3	
Density, ρ [kg/m^3]		7850	
Moment, M_1 [Nm]		372	
Number of rotation steps, n_{rot}		10	

The effects of the parameters L_c, H_c, and FE mesh density n_{mesh} on the behavior of the model were studied. The used FE mesh parameters, which define the dense part of the FE mesh (Fig. 5), are shown in Table 2.

Table 2. Parameters for the dense part of the FE mesh.

Case	2D model	3D model	Reference case for 3D model
n_{mesh}	10 – 100	10	25
n_{side}	2	2	2
b_{side}	6	6	25
c_{side}	2	2	2
n_{axial}	-	28 – 400	400

At the first stage, the 2D cylindrical bodies were considered. The stress distribution was strongly distorted in the area of interest if too small value of the parameters H_c and L_c were used. This distortion was mainly caused by the difference between the sizes of the elements between the two parts (dense and coarse) of the FE mesh. The reasonably smooth shear stress distribution was obtained with parameters H_c = 3**b* and L_c = 9**b*, as shown in Fig. 8. Dimension *b* is the half of the contact width that Hertzian theory predicts.

It is important to point out that the shape of the stress distribution in the core area (Fig. 8) corresponds very well to the analytical solution of the contact between two parallel cylinders, see [11].

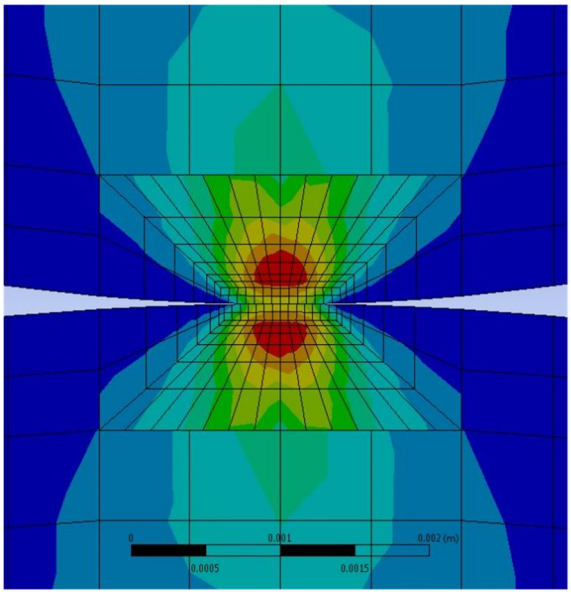

*Fig. 8. The maximum shear stress distribution with parameters H_c = 3*b, L_c = 9*b, and n_{mesh} = 10.*

The detailed effects of parameters H_c and L_c with n_{mesh} = 10 were studied and compared with the theoretical values which were calculated using Hertzian theory. The studies showed that L_c has only minor effects on the examined quantities in the core region in a range of 3**b* to 9**b*. The variation of the maximum pressure was very small with every value of H_c (1**b to* 3**b*) when the FE and analytical results were compared. However, the calculated values of the maximum shear stress and the Von Mises stress sharpen clearly towards the analytical values when H_c was increased. The comparison of the examined quantities to corresponding Hertzian results using n_{mesh} = 10 is shown in Table 3.

*Table 3. The differences (%) of the examined quantities compared to the theoretical results, H_c =3*b, L_c =9*b.*

Case	*2D model,* n_{mesh} = 10	Theoretical (Hertzian)
Maximum Pressure	-1.3%	1886 [MPa]
Maximum Von Mises	3.2%	1052 [MPa]
Maximum Shear Stress	3.4%	566.4 [MPa]
Half of the contact width, *b*	7.2%	0.2695 [mm]

In conclusion, the FE mesh worked well with 2D cylindrical bodies. Sufficient accuracy of the stresses was achieved when H_c = 3**b* and L_c = 9**b*. A very good accuracy of the maximum pressure is obtained with low number of elements in contact (n_{mesh} = 10). The maximum shear and Von Mises stresses corresponded also reasonable well with Hertzian values. However, the accuracy of the half of the contact width *b* and the position of the maximum value of the maximum shear stress are directly dependent on the element size. If these quantities are desired to be determined accurately, the FE mesh must be made denser in the core region.

Three-dimensional contact of cylindrical bodies

The effect of the FE mesh density in the axial direction on the maximum shear stress and the contact pressure was studied using 3D model. The 3D model was created by extruding the 2D model in the x-direction. The parameters of the FE mesh are shown in Table 2. The size of the dense part of the FE mesh were chosen as H_c = 3**b*, L_c = 9**b* and the number of elements in contact n_{mesh} = 10.

The maximum shear stress and the contact pressure distributions were calculated with several different values of the parameter n_{axial}. The results with two different numbers of elements in the axial direction are shown in Fig. 9.

Fig. 9 shows that the clearest differences of the stress distributions appears at the edge of the cylinder where the high number of elements is able to describe the rapid change of the stress distribution in the axial direction in more detail. It is important to note that with low number of elements (28) in the axial direction the element shapes become already very distorted and, in general, it is not the recommended way of doing the analysis. However, in this work the one objective was to develop a fast model, so it was important to study how low number of elements gives the results which are accurate enough.

The maximum shear stress and the contact pressure distributions were analyzed with several different values of the parameter n_{axial} and the results were compared to a reference case. The reference case was calculated using high amount of elements so that the element quality was good in the area of interest i.e. the number of elements in all direction was increased. The used FE mesh parameters for the reference case are shown in Table 2. With those FE mesh parameters, the quality of the elements in core area varied from 0.59 to 0.93 and the quality in contact was about 0.85. The best possible quality ratio is one [14]. The qualities of the elements and variations in the examined quantities are shown in Table 4.

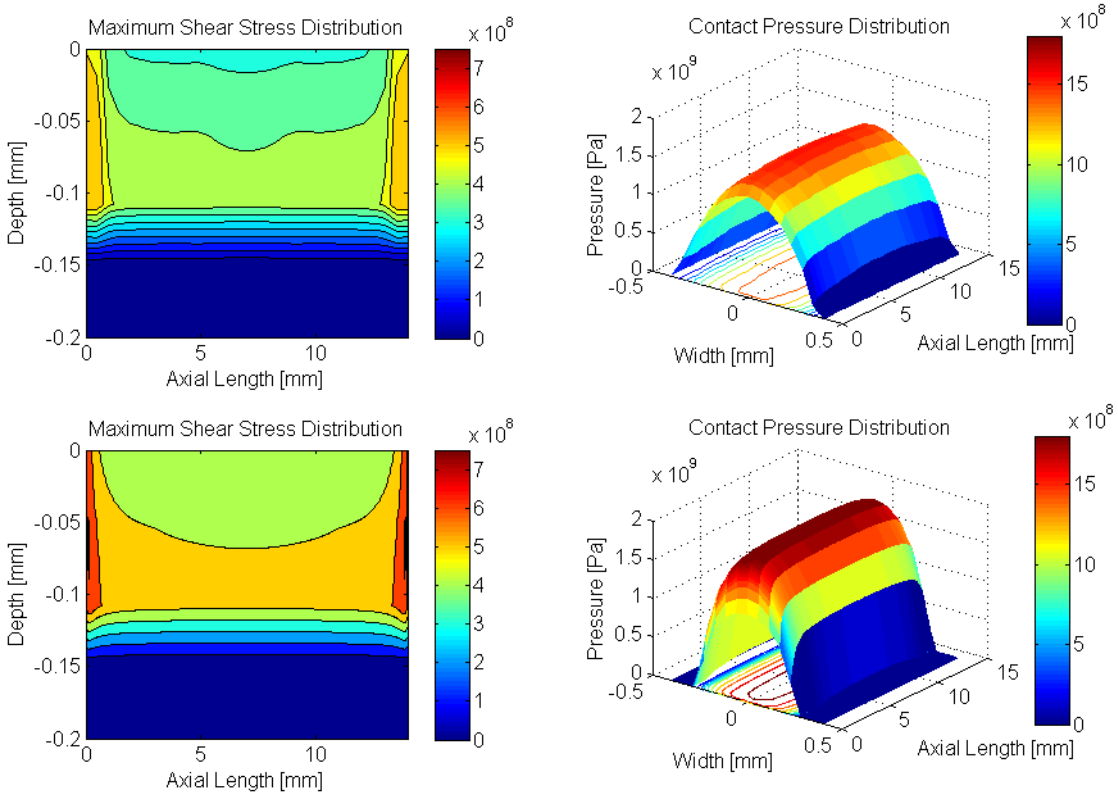

Fig. 9. The maximum shear stress distribution (axial direction at middle plane e.i. width = 0) and contact pressure distribution with n_{axial} = 28 (up-left and up-right) and n_{axial} = 400 (down-left and down-right).

Table 4. The qualities of the elements and the differences of the studied quantities compared to the reference case.

Case	n_{axial} = 100	n_{axial} = 140	n_{axial} = 400	**reference**
Qualities in core area	0.38 – 0.91	0.54 – 0.95	0.35 – 0.87	**0.59 – 0.93**
Quality in contact	0.55	0.78	0.87	**0.85**
Difference of the maximum contact pressure [%]	-8.6	-3.1	0.7	-
Differences of the contact pressure value at the edge [%]	10.9	9.3	-0.9	-
Difference of the maximum shear stress [%]	-7.8	-3.4	0.2	-

The maximum contact pressure is located in the middle of the cylinder in the length direction and it grows rapidly with increasing number of elements up to 140 elements in the axial direction. After that, it increases more steadily from about -4% to about 1% compared to the reference case. The contact pressure at the edge of the cylinder decreased fairly steadily when the number of elements, n_{axial}, increased. In addition, the maximum shear stress with n_{axial} = 140 correspond relatively well with the reference case. The very equal results was obtained with the reference and n_{axial} = 400 cases even the n_{axial} = 400 case included considerable less elements in contact region.

In conclusion, the dense FE mesh with size of H_c = 3**b*, L_c = 9**b*, and n_{mesh} = 10 combined with about 140 elements in the axial direction seems to give the reasonable accuracy in gear contact in this examined case. The differences of these calculated maximum contact pressure and shear stress values are about 4% smaller than the corresponding values calculated with the overall dense reference case.

Spur gear model comparison to analytical approaches

The results from the spur gear model were compared to the analytical approach, based on gear standard ISO 6336 [15] related to gear load capacity. In addition, the results were compared to the analytical approach in which the deformation of the meshing of gear pairs was calculated according to Weber and Banaschek [16]. Commercial gear calculation software KISSsoft [17] was used to calculate both of the reference cases. The examined quantities were the contact pressure and tooth root stresses. Common gear data for a spur gear drive and other input parameters are presented in Table 1.

To achieve an accurate enough and fast model the FE mesh parameters were chosen as follows: H_c = 3**b*, L_c = 9*b, n_{mesh} = 10, n_{side} = 2, b_{side} = 6, and c_{side} = 2. Calculation was done with two different number of elements in axial direction, n_{axial} = 100 and n_{axial} = 140. Ten contact points (rotation steps) along the line of action were calculated as a function of the angle of rotation. The angle of rotation was chosen so that only one tooth pair was in contact.

The calculation time was about 13 minutes with n_{axial} = 100 and about 16 minutes with n_{axial} = 140. The calculation was made with Dell OptiPlex 9020 workstation in which has Intel® Core™ i7-4770 Quad-Core processor, CPU speed 3.40 GHz, 16GB memory, and operating system was 64-bit Windows 7 Enterprise.

In Table 5, the results calculated with the developed spur gear model are compared to the results calculated according to the gear standard ISO 6336. It can be seen from that the values calculated with the FE model correspond relatively well to the corresponding values calculated according to the gear standard ISO 6336 Method B. The FE model gives slightly lower values than the gear standard. It is obvious that the changes of the dense part have negligible effects on the tooth root stresses as can be seen in Table 5.

The results of the maximum contact pressure calculated with the FE model and the commercial gear calculation software (reference case) are shown in Fig. 10 (a). The maximum contact pressure is presented as a function of the angle of rotation.

Table 5. The differences (%) of the results between the developed spur gear model and the gear standard ISO 6336 Method B.

Calculation method	FEM (n_{axial} = 100)	FEM (n_{axial} =140)	ISO 6336 Method B
Max contact pressure	-4.8%	-1.2%	1843 [MPa]
Max tooth root stress, pinion	-5.9%	-5.9%	515.3 [MPa]
Max tooth root stress, gear	-6.8%	-6.8%	499.8 [MPa]

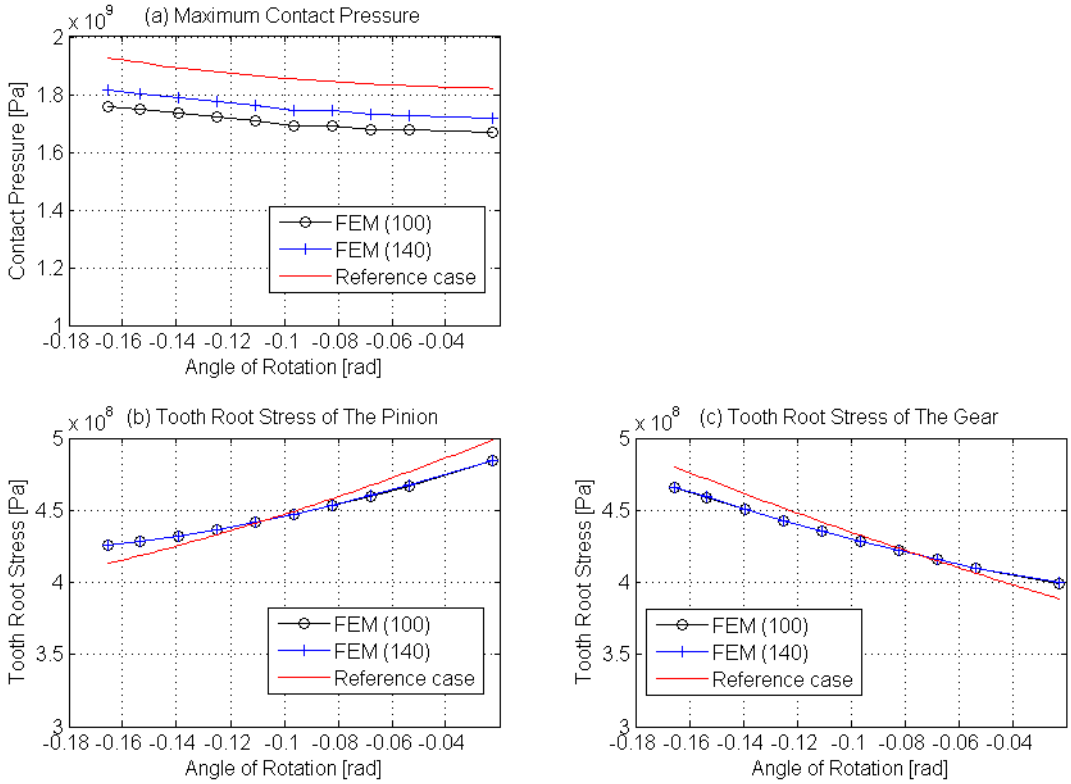

Fig. 10. The maximum contact pressure as a function of the angle of rotation (up-left); Tooth root stress of the pinion (down-left); Tooth root stress of the gear (down-right)

It can be seen from Fig. 10 (a) that the values calculated with the FE model correspond relatively well to the corresponding values obtained with commercial gear calculation software. The maximum difference is about 6% when n_{axial} = 140. The maximum contact pressure value is found in the instant position when the one pair of teeth will be taking the entire load. This point is called the highest point of single-tooth contact (HPSTC).

The corresponding comparisons of the tooth root stress of the pinion and gear are shown in Fig. 10 (b) and (c), respectively. The maximum tooth root stress was searched from each rotation step. The Fig. 10 (b) and (c) show that the developed spur gear model give almost the same results of the tooth root stress values with parameters n_{axial} = 100 and n_{axial} = 140, which corresponds to the observations made from Table 5. The

maximum difference of the tooth root stress of the pinion is about 4% and the maximum difference of the tooth root stress of the gear is about 3% compared to reference case. The deeper analysis of these differences was not in the primary scope of this study.

DISCUSSION

It is good to note that the load affects the number of elements in contact (n_{mesh}) because the dimensions of the contact area increase with the load. For this reason, the parameter n_{mesh} must be reset for each case. In addition, the dimension of the face width (b_{width}) affects the number of elements in face width direction (n_{axial}). When b_{width} increases, more elements are needed to cover the whole width to achieve the same accuracy than with thinner tooth. Correspondingly, the other dimensions of the gears affect the number of elements needed to cover the whole tooth of the gear. In general, the gear dimensions and the load affect to the selection of the FE mesh parameters. Furthermore, it is important to note that accurate solution needs enough elements in contact and in whole model, but using too many elements would result in a slow solution.

Dense FE mesh around the contact point allows the analysis of local pressure and stress behavior, which are the fundamental parameters for the basic dimensioning of the tribological contact in terms of performance and life as is also shown in gear standards. In this study a frictionless contact was assumed; even it is known that sliding is involved in gear meshing and thus tangential traction. However, in good lubrication conditions the friction coefficient in gear contact is fairly low, at the level of 0.05 [18], which contribution to shear stresses are still quite small and thus this assumption is reasonable to the basic gear contact analysis. For the advanced gear contact analysis targeting for the detailed tribological contact performance items such as flank surface roughness, (mixed) lubrication friction and friction induced temperature should be taken into account. The described model provides the basis for that kind of model development.

CONCLUSIONS

An effective parameterized model for the analysis of stresses in gear contact and gear root was developed. The main idea and feature of the contact model was to use a local adaptive finite element (FE) mesh, which moves with the point of contact along the line of action. This enabled a dense FE mesh around the contact point and a sparse FE mesh elsewhere, which resulted in a faster model with reasonable accuracy. The adaptive FE mesh, rotation of gear pair and the accurate surface profile was created in Matlab environment to obtain a good control of the flank profile and meshing parameters. These were integrated with commercial finite element method (FEM) to calculate the deformations and stress distributions. An accurate surface profile of the gear tooth flank was created by simulating the gear manufacturing i.e. the hobbing process.

The parameterization of the model was important because needed mesh density is case dependent. Tooth dimensions and loading affect to the selection of the FE mesh parameters. For example, different loading conditions may not be properly solved with

the same mesh density, because the contact area between the pinion and gear is dependent on normal load.

The developed FE mesh approach was validated successfully against analytical Hertzian theory using 2D contact of cylindrical bodies. The size of the dense part of the FE mesh, mesh density, and element shape (element distortion) were systematically studied with 2D and 3D cylindrical bodies and the proper mesh parameters were concluded. The maximum pressure converged to the high precision already with low number of elements in contact, but fairly dense FE mesh is needed to define the exact position of the maximum shear stress and the half of the contact width.

The spur gear model was compared to the analytical approach, based on gear standard ISO 6336 related to gear load capacity. In addition, the model results were compared to the analytical approach based on Weber and Banaschek by using commercial gear calculation software. Contact points including one teeth pair engagement along the line of action were calculated. The maximum contact pressure and tooth root stresses corresponded relatively well to each other with maximum differences of 1–7%.

ACKNOWLEDGEMENTS

This study was part of the FIMECC BSA programme. We gratefully acknowledge the financial support from Tekes and the participating companies: Ovako Imatra Oy Ab, Moventas Gears, and ATA Gears Ltd. CSC – IT Center for Science Ltd is thanked for providing the software used in this study.

REFERENCES

1. Litvin, F.L., Lu, J., Townsend, D.P. & Hawkins, M. Computerized Simulation of Meshing of Conventional Helical Involute Gears and Modification of Geometry. 34(1999), pp. 123–147.
2. Hedlund, J. & Lehtovaara, A. Modeling of helical gear contact with tooth deflection. Tribology International 40(2007)4, pp. 613–619.
3. Hedlund, J. & Lehtovaara, A. A parameterized numerical method for generating discrete helical gear tooth surface allowing non-standard geometry. Proceedings of the Institution of Mechanical Engineers, Part C: Journal of Mechanical Engineering Science 222(2008)6, pp. 1033–1038.
4. Ebrahimi, S. & Eberhard, P. Rigid-elastic modeling of meshing gear wheels in multibody systems. Multibody System Dynamics 16(2006)1, pp. 55–71.
5. Do, T.P., Ziegler, P. & Eberhard, P. Simulation of elastic gears with Non-standard flank profiles. Archive of Mechanical Engineering 60(2013)1, pp. 55–73.
6. Gonzalez-Perez, I., Iserte, J.L. & Fuentes, A. Implementation of Hertz theory and validation of a finite element model for stress analysis of gear drives with localized bearing contact. Mechanism and Machine Theory 46(2011)6, pp. 765–783.
7. Barbieri, M., Zippo, A. & Pellicano, F. Adaptive grid-size finite element modeling of helical gear pairs. Mechanism and Machine Theory 82(2014), pp. 17–32.
8. Litvin, F.L. & Fuentes, A. Gear geometry and applied theory. 2nd ed. New York 2004, Cambridge University Press.
9. SFS 3094 Hammaspyörät. Lieriö-hammaspyörät. Päähelpotukseton perus-profiili. Evolventtihammastus. Helsinki 1974, Suomen standardisoimisliitto.

10. Johnson, K.L. Contact Mechanics. Cambridge 1987, Cambridge University Press.
11. Stachowiak, G.W. & Batchelor, A.W. Engineering tribology. Amsterdam 1993, Elsevier science publishers.
12. Mechanical APDL Theory Reference. U.S.A 2013, ANSYS, Inc.
13. Hedlund, J. A numerical model and testing method for the evaluation of parametric excitation of cylindrical gears with shafts and bearings. Dissertation. Tampere University of Technology, Tampere 2006.
14. Meshing user's guide. U.S.A 2013, ANSYS, Inc.
15. ISO 6336 Calculation of load capasity of spur and helical gears. Switzerland 1996, International Organization for Standardization.
16. Weber, C. & Banaschek, K. Formänderung und Profilrücknahme bei gerad- und schrägverzahnten Rädern. Braunschweig 1953, Vieweg.
17. [KISSsoft (Release 03/2015D) [Computer program]. Available at http://kisssoft.com/english/home/index.php. .
18. Kleemola, J. & Lehtovaara, A. Experimental simulation of gear contact along the line of action. Tribology International 42(2009)10, pp. 1453–1459.